

On the Nature of the Lewis Acid Sites of Aluminum-Modified Silica. A Theoretical and Experimental Study

José M. Fraile, José I. García,*[†] José A. Mayoral,* Elisabet Pires, Luis Salvatella, and Miguel Ten

Departamento de Química Orgánica, Instituto de Ciencia de Materiales de Aragón, Facultad de Ciencias, C.S.I.C.-Universidad de Zaragoza, E-50009 Zaragoza, Spain

Received: September 28, 1998; In Final Form: January 5, 1999

The structures and relative Lewis acidities of the catalytic sites of four aluminum-modified silicas have been studied by means of theoretical calculations on model compounds, as well as by spectroscopic and catalytic experiments. Theoretical calculations indicate that the silica treated with Et_2AlCl has aluminum sites that are more acidic than those of AlCl_3 . The thermic treatment of the aluminum-modified silicas leads to the appearance of new, very strong acidic sites, as shown by infrared and reactivity experiments. A possible structure for these sites is proposed on the basis of the theoretical calculations.

Introduction

Solids with strong Lewis acidity are very interesting as potential substitutes for classical liquid-phase acids as catalysts of many organic reactions. It is well-known that the use of solid catalysts leads to an easy separation of the reaction products, to a reduction in the amount of effluent, and in some cases, to the recovery and reuse of the catalyst.

In this regard, the solid obtained by treating amorphous silica with Et_2AlCl has proved to give an excellent heterogeneous catalyst for a variety of Diels–Alder reactions.^{1–7} Notably, this catalyst can be stored in the open air and it is recoverable, keeping a large part of its catalytic activity,² a fact that is unusual in aluminum-derived Lewis acids. Furthermore, it has been shown that this catalyst can be efficiently used to promote some Diels–Alder reactions that either do not take place in the presence of conventional Lewis acids⁸ or take place with poor selectivities.^{9–12}

Given the practical usefulness of this solid Lewis acid, gaining knowledge about the nature of the catalytic centers becomes a particularly interesting pursuit. On the basis of theoretical results,¹³ the presence of dimeric aluminum species in the freshly prepared catalyst has been proposed. However, this kind of center is unstable and must disappear when the catalyst is used or aged, which has been related to the changes in catalytic activity experimentally observed.¹³ The principal stable catalytic centers proposed come from the reaction of Et_2AlCl with two silanol groups of the silica surface, leading to a cyclic structure in which the aluminum atom remains bonded to the chlorine atom. Ab initio calculations on simple models of the catalyst indicate that such centers have an acidity comparable to that of AlCl_3 .

Recently, in the course of a study of the CO adsorption of this catalyst at different temperatures,¹⁴ it has been shown that stronger Lewis acid sites appear when the catalyst is heated above 673 K, which adds new possibilities to the use of this solid Lewis acid.

Therefore, we decided to gain a deeper insight into the nature of the catalytic centers of silica modified with aluminum

derivatives by considering both theoretical and experimental (IR spectroscopy and catalytic activity) approaches.

Experimental Section

Computational Methods. Semiempirical calculations were carried out using the MNDO Hamiltonian,¹⁵ as implemented in the MOPAC 6.0 program.¹⁶ All the ab initio theoretical calculations described in this work were carried out using the Gaussian 94 program.¹⁷ The standard 3-21G, 3-21G(d), and 6-31G(d) basis sets were used at two different theory levels: restricted Hartree–Fock (RHF) [3-21G, 3-21G(d), and 6-31G(d)] and DFT [only with the 6-31G(d) basis set], using the three-parameter hybrid functional developed by Becke.¹⁸ The latter calculations were performed in the formulation implemented in the Gaussian 94 program (B3LYP), which is slightly different from the original proposed by Becke.

Preparation of the Catalysts. The catalysts were prepared as previously described,² using 1 M Et_2AlCl in hexane for SiAlCl and 2 M Me_3Al in hexane for SiAl . The freshly prepared catalysts were activated prior to use under vacuum at 393 K overnight (SiAlCl -393 and SiAl -393) or at 723 K for 15 h (heating rate: 1 K min^{-1}) (SiAlCl -723 and SiAl -723).

Characterization of the Catalysts. The aluminum content was determined by plasma emission spectroscopy using a Perkin-Elmer Plasma 40 emission spectrophotometer. The chlorine content was determined by conductimetry of the solution obtained after treatment of the samples with NaHCO_3 . Surface areas were determined by BET nitrogen adsorption isotherms using a Micrometrics Flowsorb 2300.

FTIR spectra were recorded using a Mattson Genesis series FTIR spectrophotometer. Self-supported wafers (20–25 mg, 12 mm diameter) were placed in a cell with NaCl windows and treated under vacuum ($<10^{-5}$ Torr) at 393 or 723 K for 1 h. Adsorption of pyridine and acetone was carried out at room temperature, and the corresponding desorption was carried out at room temperature, 323 K, and 413 K in all cases.

Diels–Alder Reactions. To a suspension of the catalyst (0.25 g, activated at 393 or 723 K) in 3.75 mL of dry toluene, under an argon atmosphere, 0.157 g of (1*R*,2*S*,5*R*)-menthyl acrylate (0.75 mmol) and then 0.050 g of freshly distilled cyclopenta-

[†] E-mail: jjg@posta.unizar.es.

TABLE 1: Specific Surfaces and Elemental Analyses of the Unmodified Silica and the Silica, Modified with Et₂AlCl and Me₃Al

solid	specific surface ^a (m ² g ⁻¹)	Al content ^b (mmol g ⁻¹)	Cl content ^c (mmol g ⁻¹)
silica	477	?	?
SiAlCl-393	340	1.68	1.78
SiAlCl-723	275	1.79	0.38
SiAl-393	280	1.90	?
SiAl-723	267	1.93	?

^a Calculated from BET nitrogen isotherms. ^b Determined by plasma emission spectroscopy. ^c Determined by conductimetry of solutions prepared from the solids.

diene (0.75 mmol) were added with a syringe. The mixture was stirred at room temperature, and the reaction was monitored by gas chromatography using the previously described method.¹⁹

In some cases the catalyst was filtered off, washed with toluene and dichloromethane, and reactivated and reused under the same conditions.

Results and Discussion

Four catalysts were considered in this study, and these came from the treatment of silica with Et₂AlCl and Me₃Al, with the resulting solids dried at 393 K (catalysts SiAlCl-393 and SiAl-393) or heated under vacuum at 723 K (catalysts SiAlCl-723 and SiAl-723). The reason for using Me₃Al was to assess the role of chlorine in the acidity of the catalysts SiAlCl-393 and SiAl-393 and to ascertain if heating at 723 K, which leads to the loss of most of the chlorine from SiAlCl-393, gives rise to similar solids irrespective of the aluminum derivative used.

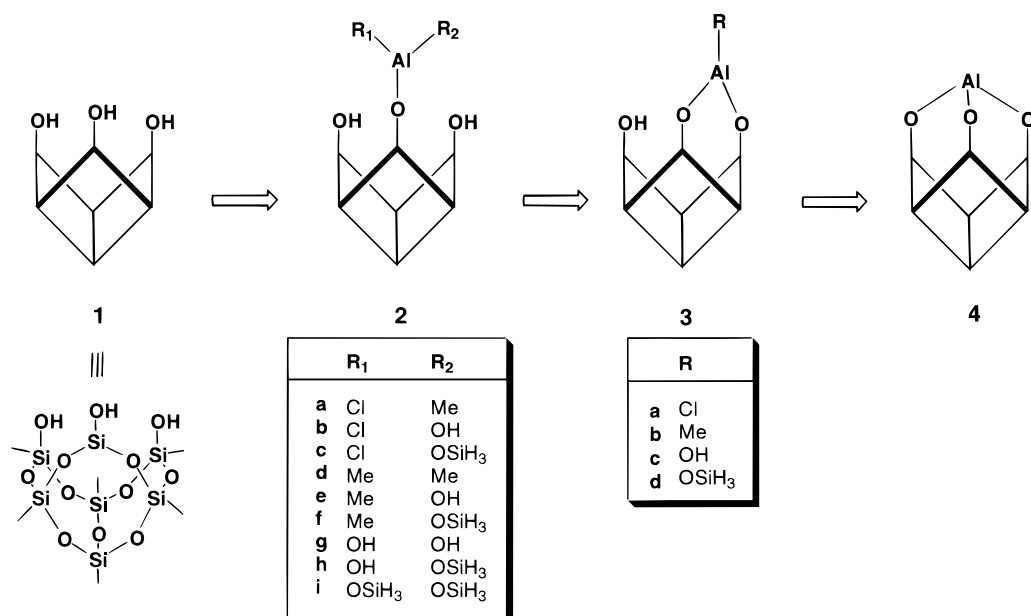
Structural and Textural Considerations. The surface areas of all the solids considered in this work were determined through the nitrogen adsorption isotherms by applying the BET theory. The results of these measurements are gathered in Table 1. As can be seen, the specific surface area decreases in the aluminum-treated silicas with regard to the unmodified silica. This effect is probably due to pore blockage caused by the grafting of the aluminum compounds. In the case of the silicas treated at 723 K, further decrease of the specific surface areas is observed,

which may be ascribed to a reorganization of the silica structure, caused by the dehydration of the superficial free silanols.

The results of aluminum and chlorine content analyses are gathered in Table 1. As can be seen, the amount of aluminum grafted onto the silica is similar, irrespective of the aluminum compound used in the treatment. Assuming the commonly accepted value of 4.5 silanol groups *per nm*²,²⁰ it can be deduced that the degree of functionalization of the silica surface is rather high and greater in the case of using Me₃Al, a molecule smaller and more reactive than Et₂AlCl. Thermic treatment of the aluminum-modified silicas always leads to an increase in the Al/surface Si ratio, which is expected, since part of the unreacted silanol groups disappear by water elimination upon heating at 723 K. In the case of SiAlCl-393, the aluminum and chlorine content is very similar, indicating that, on average, each aluminum center retains the chlorine atom present in the starting aluminum compound, Et₂AlCl. It is worth noting that, in the case of the SiAlCl-723 solid, a significant amount of chlorine remains after the thermic treatment. This indicates that some of the aluminum–chlorine bonds are highly resistant, probably owing to the lack of nearby silanol groups able to participate in the loss of chlorine through the formation of hydrogen chloride.

Theoretical Study. Prior to building models for the catalytic aluminum sites, it was important to have a good starting model for the silica surface. It has been reported²¹ that the trisilanol **1**, shown in Scheme 1, bears a similarity to the potential coordination sites of several forms of SiO₂, and thus, it is a good model for the silica surface. Moreover, by virtue of these similarities, one can expect that the metallasiloxanes derived from this silanol would serve as model systems for many heterogeneous silica-supported catalyst systems.²²

Indeed, very recently, growing interest has been shown in the use of silsesquioxanes as experimental models of silica, aluminosilicates, and silica-supported catalysts.^{22–25} However, to the best of our knowledge, the use of these kinds of structures as theoretical models of catalytic sites has not yet been attempted. Only very recently, cage-like clusters of the hydridosilsesquioxane type have been used as theoretical models to mimic the isolated hydroxyl groups of silica in DFT computation of

SCHEME 1

the vibrational modes of the Si—OH group.²⁶ Therefore, we decided to use a simplified version of trisilanol **1**, namely, that in which the cyclohexyl groups have been replaced by hydrogen atoms, as a model of the silica surface, and from this starting point, we constructed the possible catalytic centers formed during the grafting of the aluminum compound, including the possibility of partial hydrolysis of the aluminum—carbon bonds. Scheme 1 shows all the possibilities considered in the present work.

The size of the resulting structures is sufficient to make the use of high-level *ab initio* calculations with inclusion of geometry optimization extremely difficult. In a previous study,¹³ we showed that MNDO geometries can be successfully used, in combination with high-level *ab initio* single-point calculations, to deal with simple models of silica-modified catalysts and to predict the relative Lewis acidities of the different catalytic sites. First of all, we began by testing whether MNDO geometries of the catalytic center models (both free and coordinated to an organic molecular probe), coupled with single-point *ab initio* calculations, are sufficient to adequately describe these systems.

To this end, the silsesquioxane structure **4** was chosen as the test structure for two main reasons. First, the X-ray structure of an aluminosilsesquioxane—OPPh₃ complex has been described,²⁷ which helps to ascertain if the calculated geometries for the reagent—catalyst complex models are realistic. Second, as we will discuss below, the structure of **4**, in which the aluminum atom participates in three eight-membered siloxane cycles, is the one that we propose as being formed by thermic treatment of the catalysts. It is therefore interesting to gain a deeper insight into this structure. Furthermore, similar structures bearing aluminum centers of high Lewis acidity have been proposed as intermediates in the process of dealumination of zeolites.²⁸

The geometry of the aluminosilsesquioxane **4** was optimized at the MNDO, HF/3-21G, HF/3-21G(d), HF/6-31G(d), and B3LYP/6-31G(d) theory levels, and a survey of geometrical parameters is shown in Figure 1. On the basis of a preliminary analysis, it can be concluded that the MNDO geometry is very similar to that calculated at the HF/3-21G level. On the other hand, as the theoretical model becomes more complicated by inclusion of polarization functions, larger-sized basis sets, and electronic correlation (through the density functional theory approach), the MNDO and *ab initio* geometries become somewhat different. In particular, the Al—O bond length (continuously increasing with the theoretical level) and the pyramidal O—Al(O)—O angle (closest to planarity at the higher theoretical level) show the most prominent differences.

A more rigorous comparison between the calculated geometries can be performed by means of superimposition of the different structures, thus minimizing the residual mean square of the Cartesian coordinate differences between the heavy atoms of both structures (Al, Si, O).²⁹ The global rms obtained when the MNDO and B3LYP/6-31G(d) geometries are compared (0.077 Å²) is quite acceptable and indicates that the former can be used for single-point calculations at higher theory levels.

The geometries of the acetone—**4** complex were also optimized at the same theoretical levels. In this case, the calculated structures can be directly compared with that of the aluminosilsesquioxane—OPPh₃ complex experimentally determined by X-ray diffraction.²⁷ Figure 2 shows some of the most significant geometrical parameters for both structures. As can be seen, MNDO performs well and, in this case, the pyramidal O—Al(O)—O angle is very close to that experimentally found for the triphenylphosphine oxide complex (129.5° vs 128°).

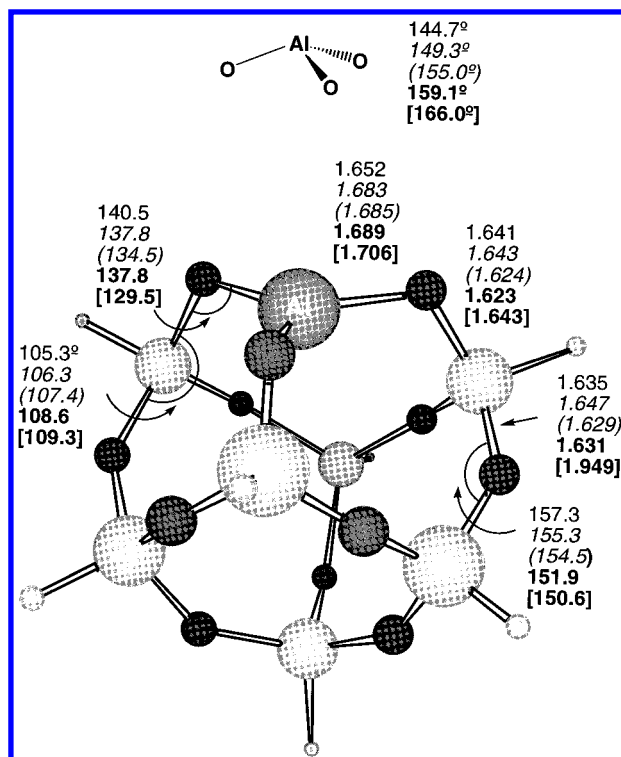


Figure 1. Selected geometrical parameters for structure **4** calculated at the MNDO (plain text), HF/3-21G (italic), HF/3-21G(d) (italic between parentheses), HF/6-31G(d) (boldface), and B3LYP/6-31G(d) (boldface between brackets) theoretical levels.

The next step was to test if the coordination energy of a probe molecule such as acetone, which we take as an acidity index, could be adequately estimated at the B3LYP/6-31G(d)/MNDO level. To this end, the corresponding coordination energies were calculated at the MNDO (−12.1 kcal mol^{−1}), HF/3-21G(d) (−58.2 kcal mol^{−1}), HF/6-31G(d) (−41.5 kcal mol^{−1}), B3LYP/6-31G(d)/MNDO (−40.8 kcal mol^{−1}), B3LYP/6-31G(d)/HF/6-31G(d) (−40.7 kcal mol^{−1}), and B3LYP/6-31G(d) (−40.4 kcal mol^{−1}) levels. As can be seen, the coordination energy calculated at the MNDO level is clearly underestimated, and that calculated at the HF/3-21G(d) level overestimated, with regard to the best theoretical estimate [−40.4 kcal mol^{−1} at the B3LYP/6-31G(d) level]. However, the rest of the calculations give energy values close to this reference energy. In particular, the B3LYP/6-31G(d)/MNDO single-point calculation leads to a coordination energy value that is quite satisfactory. It is worth noting that the B3LYP/6-31G(d)/MNDO and the B3LYP/6-31G(d)/HF/6-31G(d) single-point calculations, as well as the full B3LYP/6-31G(d) calculation, lead to almost identical energy values, indicating that the small geometric differences calculated at these levels are not relevant to the study of the acidity of the aluminum center. Therefore, the use of the B3LYP/6-31G(d)/MNDO theoretical level seems to be justified and represents an excellent compromise between computational cost and chemical accuracy.

The next step was to model the different aluminum centers that can be formed by treatment of the silica with Me₂AlCl (taken as a model of Et₂AlCl) and Me₃Al. The resulting structures are shown in Scheme 1.

Structures **2** come from the reaction of the aluminum compound with only one silanol group of the silica surface. Apart from the “direct” structures coming from the elimination of methane or hydrogen chloride (**2a** and **2d**), we have also considered the possibility of the partial or total hydrolysis of the Al—Cl or Al—CH₃ bonds (**2b**, **2e**, and **2g**). To consider the influence of the geometrical constraints imposed by the tricyclic

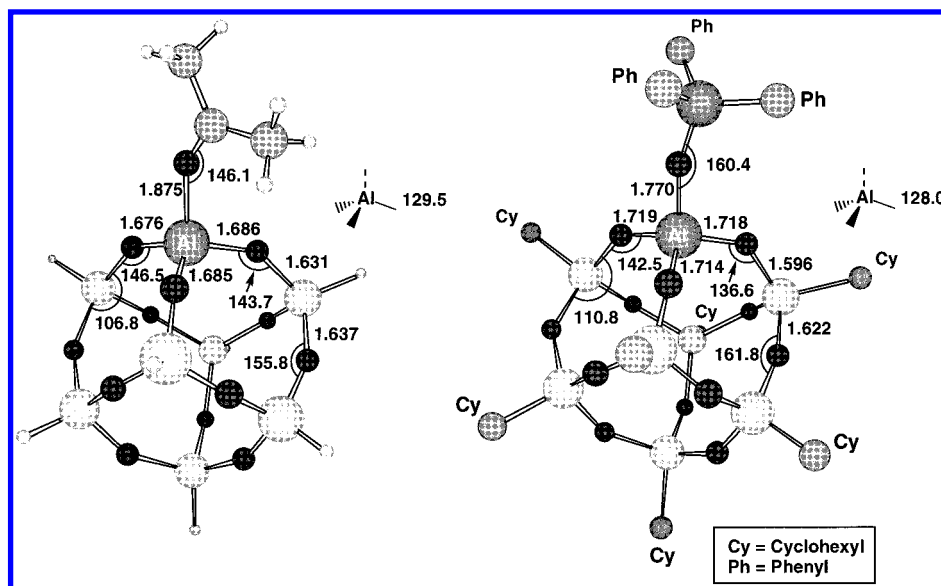


Figure 2. Comparison between calculated (MNDO) geometrical parameters for the acetone–4 complex and the experimental (X-ray) geometry of a triphenylphosphine oxide–aluminosilsesquioxane complex.

TABLE 2: Calculated (B3LYP/6-31G(d)//MNDO) Absolute (in hartree) and Coordination (in kcal mol⁻¹) Energies of the Catalytic Center Models and Their Respective Complexes with Acetone

model	R ₁	R ₂	<i>E</i> _{model}	<i>E</i> _{complex}	Δ <i>E</i>
2a	Cl	CH ₃	-3678.2293	-3871.4323	-25.0
2b	Cl	OH	-3174.2699	-3907.3822	-26.2
2c	Cl	OSiH ₃	-4005.0000	-4198.1169	-29.1
2d	CH ₃	CH ₃	-3257.8717	-3451.0628	-23.3
2e	CH ₃	OH	-3293.8299	-3487.0180	-21.4
2f	CH ₃	OSiH ₃	-3584.5600	-3777.7580	-24.1
2g	OH	OH	-3329.8622	-3522.9804	-22.5
2h	OH	OSiH ₃	-3620.5221	-3813.7203	-27.7
2i	OSiH ₃	OSiH ₃	-3911.2420	-4104.4414	-28.4
3a	Cl		-3637.7731	-3830.9821	-34.4
3b	CH ₃		-3217.4272	-3410.6230	-26.2
3c	OH		-3253.3829	-3446.5854	-30.4
3d	OSiH ₃		-3544.1107	-3737.3114	-29.2
4			-3176.9559	-3370.1750	-40.8
AlCl ₃			-1623.2327	-1816.4350	-30.2

structure of the trisilanol **1** (see below), we have also considered some structures “end-capped” with silane groups (**2c**, **2f**, **2h**, and **2i**).

Structures **3** come from the reaction of the grafted aluminum compound with a second silanol group of the silica surface. Again, besides the direct structures (**3a** and **3b**), we have also considered the hydrolyzed (**3c**) and silanized (**3d**) possibilities. Finally, structure **4** would arise from the reaction of the grafted aluminum compound with a third neighboring silanol group. Such a process closes the structure, giving rise to an aluminosilsesquioxane.

All these structures, as well as their corresponding complexes with acetone, were optimized using the semiempirical MNDO Hamiltonian, and then single-point energy calculations were carried out at the DFT B3LYP/6-31G(d) theory level. The calculated total and complexation energies are given in Table 2.

First of all, let us consider those catalytic centers directly formed by reaction of the aluminum derivative (Me₂AlCl or Me₃Al) with the silica surface, i.e., **2a**, **2d**, **3a**, **3b**, and **4**. As expected, the chlorine atom enhances the acidity of the aluminum center. Thus, the order of acidity (as expressed by the complexation energy with acetone) is **2a** > **2d**, and **3a** > **3b**. It is worth noting that the acidity of the aluminum center in

3a is greater than that calculated for AlCl₃ at the same theoretical level (−30.2 kcal mol⁻¹).

Structural features also play a role in determining the final acidity of the aluminum center. Thus, **3a** is more acidic than its analogue **2c**, and **3b** is more acidic than **2f**. This seems to indicate that the structural rigidity introduced by the eight-membered ring in which the aluminum atom participates is a key factor to enhance its acidity. This hypothesis is confirmed by the extraordinarily high acidity of **4** (−40.8 kcal mol⁻¹). In this structure, the aluminum atom simultaneously participates in three rings, leading to the closure of the silsesquioxane structure. By comparison, the analogous structures of **2i** and **3d** (three O–Si bonds around the aluminum atom) are much less acidic (−28.4 and −29.2 kcal mol⁻¹, respectively), the latter being in turn somewhat more acidic than the former.

As a conclusion, the most acidic center that can be formed by grafting an aluminum derivative onto silica is that modeled by structure **4**. However, this requires a particular disposition of three silanol groups at a suitable distance. We propose that this kind of acidic site is mostly produced during the thermic treatment of the modified silicas. We will return to this point below.

The treatment of silica with Me₂AlCl can give rise to a variety of acidic centers (**2a**, **3a**, and **3b**, only considering direct substitutions). Of these, **3a** is the most acidic center and is even more acidic than AlCl₃. The presence of one chlorine atom per aluminum atom found by elemental analysis, as well as the estimated Al/surface Si ratio, supports the hypothesis that catalytic centers of type **3a** are the most probable. It is worth noting that the eventual hydrolysis or silanolysis of the chlorine–aluminum bond would lead to structures **3c** and **3d**, which both still have an acidity comparable to that of AlCl₃. This could help to explain the exceptional behavior of this solid aluminum catalyst, which can be stored open to the atmosphere and recovered, keeping most of its catalytic activity.

The treatment of silica with Me₃Al gives rise to acidic centers of types **2d** and **3b**. These centers are much less acidic than those arising from the treatment with Me₂AlCl, and therefore, one would expect the resulting silicas to be poorer catalysts. On the other hand, the thermal treatment would lead to centers of type **4**, and then the two aluminum-treated silicas should behave similarly after the thermic treatment. Spectroscopic and

TABLE 3: Brønsted and Lewis IR Bands of Pyridine Adsorbed onto Aluminum-Modified Silicas

solid	Brønsted		Lewis		L/B ^a
	ν (cm ⁻¹)	relative integral	ν (cm ⁻¹)	relative integral	
SiAlCl-393	1549	1.00	1452	5.30	5.3
SiAl-393	1553	0.13	1454	4.27	32.0
SiAlCl-723	1550	0.30	1450	4.70	15.7
SiAl-723	1552	0.47	1552	4.20	9.0

^a Ratio of integral areas.

catalytic experiments can help to ascertain the validity of these hypotheses, and these will be discussed in the following sections.

Infrared Spectroscopy Experiments. The aluminum-modified silicas were characterized by IR spectroscopy of molecular probes adsorbed onto the solids.

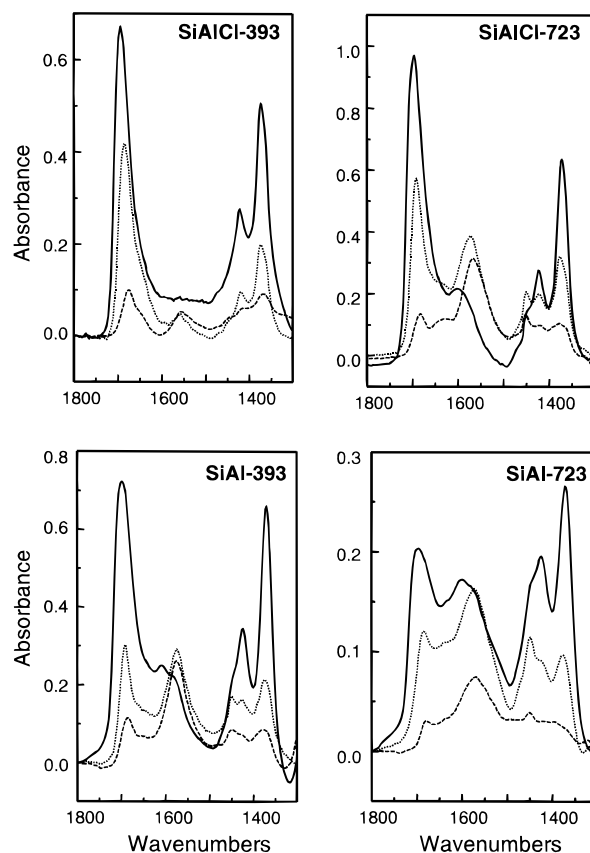
Pyridine adsorption–desorption experiments were carried out in order to determine the relative proportion of Lewis and Brønsted acidic sites. The numerical data of the spectra for desorption at 413 K are given in Table 3. The integral areas of the Lewis and Brønsted bands were normalized with regard to the structural bands of the silica between 1800 and 2100 cm⁻¹.

As can be seen, all the solids are mainly Lewis acids, with Lewis/Brønsted band ratios (L/B) of 5 or more. The band ratio is nearly the same as the site ratio, as indicated by calculations using the extinction coefficients of Brønsted and Lewis sites in the common band at 1490 cm⁻¹. SiAlCl-393 shows the highest Brønsted acidity, which may be because of the polarization of residual water (not completely eliminated by heating at 393 K) bonded to the strong Al–Cl Lewis acid sites. Of particular interest is the solid SiAl-393, which has an exceptionally low Brønsted acidity that leads to the higher L/B ratio determined for this series. The thermic treatment of SiAlCl-393 and SiAl-393 leads to different relative effects. In the former case, there is a clear decrease in the number and relative proportion of Brønsted acid sites, and this leads to an increase in the L/B ratio. In the second case, the number and proportion of these sites increase, leading to a decrease in the L/B ratio. It is worth noting, however, that both SiAlCl-723 and SiAl-723 are much more similar to each other than SiAlCl-393 and SiAl-393, which indicates that the thermic treatment of the aluminum-treated silicas leads to solids of similar characteristics irrespective of the aluminum compound used.

Acetone also was used as a molecular probe in adsorption–desorption IR experiments. Since acetone is a much weaker basic probe, it cannot easily be used to distinguish between Brønsted and Lewis acid sites. Furthermore, there is an additional complication in the use of acetone as a molecular probe, namely, its relative ease of self-condensation to give mesityl oxide, a process that is catalyzed by acid centers. The presence of mesityl oxide can be detected by the appearance of a conjugated C=C band in the range 1550–1600 cm⁻¹.³⁰

The features of IR spectra of acetone and mesityl oxide, adsorbed onto different solid acids, have recently been studied in detail by Panov and Fripiat.^{30,31} As these authors observed, the self-condensation of acetone to give mesityl oxide is mainly catalyzed by the Lewis acid centers so that the rate of appearance of this byproduct can also serve as a probe for the presence and/or strength of such sites.

Figure 3 shows the spectra of acetone adsorbed onto the aluminum-modified silicas and then desorbed at room temperature, at 323 K, and at 413 K. The corresponding numerical data of the deconvoluted spectra are given in Table 4. As can be seen from these data, all the solids display two types of

**Figure 3.** IR spectra of acetone adsorbed onto aluminum-modified silicas and desorbed at room temperature (continuous line), 323 K (dotted line), and 413 K (dashed line).**TABLE 4: IR Bands^a of Acetone and Mesityl Oxide Adsorbed onto Aluminum-Modified Silicas and Desorbed at Several Temperatures**

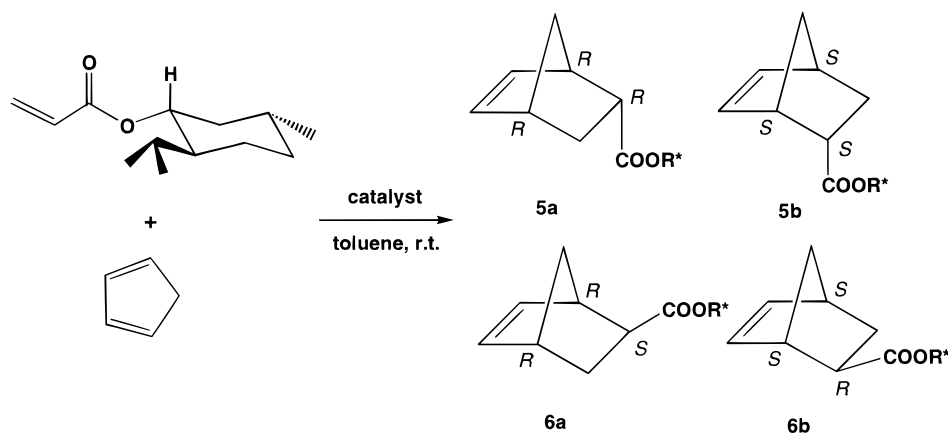
catalyst	desorption <i>T</i> (K)	$\nu_{\text{C=O}}$ (cm ⁻¹)	$\nu_{\text{C=C}}$ (cm ⁻¹)
SiAlCl-393	rt	1694	1667
	323	1686	1657
	413	1676	1643
SiAl-393	rt	1706	1690
	323	1693	1668
	413	1687	1655
SiAlCl-723	rt	1701	1681
	323	1691	1656
	413	1684	1638
SiAl-723	rt	1707	1687
	323	1687	1665
	413	1680	1646

^a Values determined by deconvolution of the original spectra.

carbonyl stretching band. For the sake of comparison, it has been reported that acetone adsorbed onto zeolites displays a band in the range 1676–1682 cm⁻¹, corresponding to a coordination to weakly acidic OH,^{30,32} whereas the band corresponding to the coordination to Lewis acid sites appears in the range 1690–1701 cm⁻¹.³⁰ All the aluminum-modified silicas show bands in this zone (1676–1707 cm⁻¹), which indicates the presence of sites of acidity similar to that of the solids described above. The range 1652–1655 cm⁻¹ corresponds to acetone interacting with strong acid sites.^{30,31} Unfortunately, this range also covers the C=O stretching vibration of adsorbed mesityl oxide^{30,31} so that in those cases in which this compound appears it is impossible to make a clear assignment of the corresponding carbonyl bands.

As can be seen in Figure 3, only SiAlCl-393 displays spectra free or almost free of mesityl oxide, at least at low desorption

SCHEME 2



temperatures. In this case, the assignment of the carbonyl bands as corresponding to adsorbed acetone is straightforward, and it can be concluded that there are at least two types of acidic center. The frequency of the second band ($1657\text{--}1667\text{ cm}^{-1}$) indicates the presence of strong acid sites in this solid. In the rest of the cases studied, the presence of mesityl oxide is observed at all desorption temperatures so that it is difficult to distinguish between the carbonyl band of the acetone coordinated to strong acid sites and that of mesityl oxide.

However, the relative intensity of the C=C band of the mesityl oxide with regard to the C=O band of the acetone coordinated to the Lewis acid sites can be used as an indicator of the nature of the acid sites of these solids. Thus, it can be observed that mesityl oxide only appears to a significant extent in the case of SiAlCl-393, when the desorption temperature is as high as 413 K. On the other hand, in the case of SiAl-393, mesityl oxide is observed even at room temperature, and indeed, it is the major product even at 313 K. This correlates well with the Lewis/Brønsted acidity ratio calculated from the pyridine adsorption experiments (Table 3). If we accept that the Lewis acid sites are the main ones responsible for the appearance of mesityl oxide,^{30,31} not only their number but also their strength should be important. Thus, with solids treated at 723 K, bearing strong type 4 sites (Scheme 1, Table 2), a higher relative concentration of mesityl oxide is observed, with regard to the same solids treated at 393 K.

Catalysis Experiments. The Diels-Alder reaction of cyclopentadiene with (1*R*,2*S*,5*R*)-menthyl acrylate (Scheme 2) was chosen as a benchmark reaction to test the catalytic properties of the aluminum-modified silicas. This reaction allows the study not only of the catalytic activity but also of two types of stereoselectivity, namely, the endo/exo and the diastereofacial (asymmetric induction) selectivities. Furthermore, this reaction had also been used in our group to establish changes in the reaction mechanism when catalyzed by heterogeneous catalysts.³³

Table 5 shows the most relevant experimental results of the catalyzed reactions. With regard to the selectivity of the reaction, it can be seen that both the endo/exo and the diastereofacial selectivities do not change very much from one catalyst to the other or with the progress of the reaction. The values observed (about 90:10 in endo/exo selectivity and 40% diastereomeric excess) are typical for this reaction when it is catalyzed by Lewis acids, so these results are indicative that all the solids tested behave as acid catalysts.

With regard to the conversion, the SiAlCl-393 catalyst is somewhat more active than SiAl-393 at the beginning of the

TABLE 5: Results of the Reaction between Cyclopentadiene and (1*R*,2*S*,5*R*)-Menthyl Acrylate, Catalyzed by Aluminum-Modified Silicas

catalyst	30 min			24 h		
	yield (%)	5/6	5a/5b	yield (%)	5/6	5a/5b
SiAlCl-393	40	93/7	69/31	57	92/8	66/34
SiAl-393	31	91/9	69/31	96	91/9	64/36
SiAlCl-723	51	92/8	73/27	75	92/8	67/33
SiAlCl-723 ^a	47	92/8	70/30	76	92/8	64/36
SiAl-723	54	92/8	70/30	79	92/8	78/22
SiAl-723 ^a	44	91/9	80/20	72	92/8	71/29

^a Recovered catalyst.

reaction, which is in good agreement with the stronger acidity of the sites 3a, bearing a chlorine atom, in comparison to 3b, which is derived from Me₃Al. However, the final conversion is higher for the latter, which is probably due to the effect of the Brønsted acid sites. These sites are able to catalyze the polymerization of the cyclopentadiene so that the reaction stops when this reagent disappears (we did not work with excess diene). This seems to be the situation in the case of SiAlCl-393 (the same conversion is observed after 2 and 24 h of reaction). As already mentioned in the preceding section, SiAl-393 has an unusually low Brønsted acidity so that the disappearance of cyclopentadiene does not take place and that the Diels-Alder reaction progresses to almost total conversion of both reagents.

Both SiAlCl-393 and SiAl-393 catalysts are less active than SiAlCl-723 and SiAl-723, which, in turn, display almost identical activities. The higher activity of the thermally treated catalysts is in good agreement with the calculations for site 4, which is the stronger acid site. The identical activities of these solids are in agreement with the IR experiments; i.e. the thermic treatment gives rise to solids of similar characteristics irrespective of the aluminum compound used. In the case of SiAl-723, the final conversion is not as high as that obtained with SiAl-393. This could be due to the increase in Brønsted acidity experienced by this solid during the course of the thermic treatment, as shown by the pyridine adsorption IR results. Some strong Brønsted acid sites, similar to those present in zeolites, may be generated by reaction of an aluminum atom of a site 4 with a fourth nearby silanol group.

It is important to note that the thermic treatment confers more stability on these solids, as demonstrated by the results obtained with the recovered catalysts. Only a slightly lower initial activity is observed, with almost identical final conversions. This result is very interesting from a practical viewpoint, given that it describes a solid Lewis acid that is fully recoverable and able

to promote asymmetric Diels–Alder reactions with fairly unreactive dienophiles, such as (1*R*,2*S*,5*R*)-menthyl acrylate, without using an excess of diene.

Conclusions

The treatment of silica gel with aluminum compounds leads to solids that display acid properties and are suitable to efficiently catalyze organic reactions. The IR and catalytic experiments indicate that the solid obtained from the treatment of silica with Et₂AlCl is a stronger Lewis acid than that obtained from the treatment with Me₃Al, which is a result of the presence of Al–Cl bonds in the solid. Theoretical calculations on models of the catalytic aluminum sites agree with this interpretation, and thus, aluminum sites bearing a chlorine atom possess a Lewis acidity higher than that calculated for AlCl₃. On the other hand, the final conversion obtained with the latter solid is higher, which is related to its exceptionally low Brønsted acidity.

The thermic treatment of both aluminum-grafted silicas leads to solids with similar physicochemical properties, as shown by spectroscopic and catalytic experiments. These solids are more active than the original ones, indicating that new, stronger acid centers are formed upon thermic treatment. We propose that these centers are similar to those formed during the partial dealumination of zeolites; i.e., the aluminum atom forms part of a tricyclic siloxane system, and this structural rigidity gives it an enhanced acidity. Theoretical calculations on a model of this kind of site agree with this hypothesis, given that the calculated acidity is by far the highest among all the possibilities considered. The high activity and reusability of these solids make them very useful as Lewis acid catalysts.

In conclusion, the combination of theoretical, spectroscopic, and catalytic experiments has proven to be a powerful tool to gain a deeper insight into the nature of the catalytic sites of aluminum modified silicas, which can be of help in the design of new and more efficient solid catalysts.

Acknowledgment. This work has been made possible by the Comisión Interministerial de Ciencia y Tecnología (Project MAT96-1053). E.P. acknowledges the Diputación General de Aragón for a predoctoral grant.

Supporting Information Available: MNDO geometries of structures **2a–i**, **3a–d**, **4** and their corresponding complexes with acetone, HF/3-21G, HF/3-21G(d), HF/6-31G(d), and B3LYP/6-31G(d) geometries of structure **4**, residual mean square values for the geometrical fit between the structures of silsesquioxane **4**, calculated at several theoretical levels, and absolute and coordination energies of the aluminosilsesquioxane **4**, acetone, and their respective complexes, calculated at several theoretical levels. This material is available free of charge via the Internet at <http://pubs.acs.org>.

References and Notes

- (1) Cativiela, C.; Figueras, F.; García, J. I.; Mayoral, J. A.; Pires, E.; Royo, A. J. *Tetrahedron: Asymmetry* **1993**, *4*, 621.
- (2) Cativiela, C.; Fraile, J. M.; García, J. I.; Mayoral, J. A.; Pires, E.; Royo, A. J.; Figueras, F.; de Mènorval, L. C. *Tetrahedron* **1993**, *49*, 4073.
- (3) Cativiela, C.; García, J. I.; Mayoral, J. A.; Pires, E.; Royo, A. J.; Figueras, F. *Tetrahedron* **1995**, *51*, 1295.
- (4) Cativiela, C.; García, J. I.; Mayoral, J. A.; Pires, E.; Royo, A. J.; Figueras, F. *Appl. Catal. A* **1995**, *131*, 159.
- (5) García, J. I.; Mayoral, J. A.; Pires, E.; Brown, D. R.; Massam, J. *Catal. Lett.* **1996**, *37*, 261.
- (6) Fraile, J. M.; García, J. I.; Mayoral, J. A.; Pires, E.; Tarnai, T.; Figueras, F. *Appl. Catal. A* **1996**, *136*, 113.
- (7) Fraile, J. M.; García, J. I.; Mayoral, J. A.; Pires, E.; Tarnai, T. *Catal. Lett.* **1998**, *51*, 235.
- (8) Fraile, J. M.; García, J. I.; Gracia, D.; Mayoral, J. A.; Pires, E. *J. Org. Chem.* **1996**, *61*, 9479.
- (9) Cativiela, C.; García, J. I.; Mayoral, J. A.; Pires, E.; Brown, R. *Tetrahedron* **1995**, *51*, 9217.
- (10) Cativiela, C.; Fraile, J. M.; García, J. I.; López, M. P.; Mayoral, J. A.; Pires, E. *Tetrahedron: Asymmetry* **1996**, *7*, 2391.
- (11) Hart, D. J.; Wu, W.-L.; Kozikowski, A. P. *J. Am. Chem. Soc.* **1996**, *117*, 9369.
- (12) Hart, D. J.; Li, J.; Wu, W.-L.; Kozikowski, A. P. *J. Org. Chem.* **1997**, *62*, 5023.
- (13) Fraile, J. M.; García, J. I.; Mayoral, J. A.; Pires, E. *J. Mol. Catal. A* **1997**, *119*, 95.
- (14) Figueras, F.; Allian, M.; Fraile, J. M.; García, J. I.; Garrone, E.; Lefevre, F.; Mayoral, J. A.; de Mènorval, L. C.; Pires, E.; Rachdie, F.; Sainz-Díaz, C. I.; Sánchez-Sierra, M. C. Submitted for publication.
- (15) Dewar, M. J. S.; Thiel, W. *J. Am. Chem. Soc.* **1977**, *99*, 4899, 4907.
- (16) Stewart, J. J. P. MOPAC 6.0. *QCPE* 455, 1990.
- (17) Frisch, M. J.; Trucks, G. W.; Schlegel, H. B.; Gill, P. M. W.; Johnson, B. G.; Robb, M. A.; Cheeseman, J. R.; Keith, T. A.; Petersson, G. A.; Montgomery, J. A.; Raghavachari, K.; Al-Latham, M. A.; Zakrzewski, V. G.; Ortiz, J. V.; Foresman, J. B.; Cioslowski, J.; Stefanov, B. B.; Nanayakara, A.; Challacombe, M.; Peng, C. Y.; Ayala, P. Y.; Chen, W.; Wong, M. W.; Andrés, J. L.; Replogle, E. S.; Gomperts, R.; Martin, R. L.; Fox, D. J.; Binkley, J. S.; Defrees, D. J.; Baker, J.; Stewart, J. J. P.; Head-Gordon, M.; González, C.; Pople, J. A. GAUSSIAN 94, revision D.3; Gaussian Inc.: Pittsburgh, PA, 1995.
- (18) Becke, A. D. *J. Chem. Phys.* **1993**, *98*, 5648. Lee, C.; Yang, W.; Parr, R. *Phys. Rev. B* **1988**, *37*, 785.
- (19) Cativiela, C.; Figueras, F.; Fraile, J. M.; García, J. I.; Mayoral, J. A. *Tetrahedron: Asymmetry* **1991**, *2*, 953.
- (20) Odhaya, M.; Scott, R. P. W.; Simpson, C. F. *J. Therm. Anal.* **1993**, *40*, 1197.
- (21) Murugavel, R.; Voigt, A.; Walawalkar, M. G.; Roesky, H. W. *Chem. Rev.* **1996**, *96*, 2205.
- (22) Feher, F. J.; Phillips, S. H.; Ziller, J. W. *Chem. Commun.* **1997**, 829.
- (23) Maschmeyer, T.; Klunduk, M. C.; Martin, C. M.; Shephard, D. S.; Thomas, J. M.; Johnson, B. F. G. *Chem. Commun.* **1997**, 1847.
- (24) Wada, K.; Nakashita, M.; Yamamoto, A.; Wada, H.; Mitsudo, T. *Chem. Lett.* **1997**, 1209.
- (25) Feher, F. J.; Soulivong, D.; Lewis, G. T. *J. Am. Chem. Soc.* **1997**, *119*, 11323.
- (26) Civalieri, B.; Garrone, E.; Ugliengo, P. *Chem. Phys. Lett.* **1998**, *294*, 103.
- (27) Feher, F. J.; Budzichowski, T. A.; Weller, K. J. *Polyhedron* **1993**, *12*, 591.
- (28) Zecchina, A.; Otero-Areán, C. *Chem. Soc. Rev.* **1996**, 187.
- (29) MacLachlan, A. D. *Acta Crystallogr.* **1972**, *A28*, 656. MacLachlan, A. D. *Acta Crystallogr.* **1982**, *A38*, 871.
- (30) Panov, A.; Fripiat, J. J. *Langmuir* **1998**, *14*, 3788.
- (31) Panov, A.; Fripiat, J. J. *J. Catal.* **1998**, *178*, 188.
- (32) Florián, J.; Kubelkova, L. *J. Phys. Chem.* **1994**, *98*, 8734.
- (33) Fraile, J. M.; García, J. I.; Gracia, D.; Mayoral, J. A.; Tarnai, T.; Figueras, F. *J. Mol. Catal. A* **1997**, *121*, 97.